Band Structure of Cadmium Sulfide—Photoemission Studies*

N. B. KINDIG† AND W. E. SPICER
Stanford Electronics Laboratories, Stanford University, Stanford, California
(Received 23 November 1964)

Photoemission measurements have been made at photon energies between 7.2 and 11.6 eV on single crystals of CdS which had been cleaved in high vacuum at pressures $<10^{-9}$ Torr. Additional measurements have been made from 6 to 21.2 eV using surfaces cleaved and tested in pressures of about 10^{-4} Torr. The electron affinities are found to be 4.8 ± 0.3 and 3.8 ± 0.4 eV for the high- and low-vacuum-cleaved samples, respectively. Important features of the density of states are deduced from the energy distributions. Maxima in the density of states are located in the conduction band at 6.7 ± 0.3, 8.2 ± 0.3 eV and (with the aid of reflectivity data) at 4.4 ± 0.5 eV. A single maximum in the valence-band density of states is found at -1.2 ± 0.3 eV and the *d* band of Cd is located at -9.4 ± 0.5 eV. All energies are referred to the top of the valence band. These features agree qualitatively with the calculated band structure of Herman and Skillman and, in the case of the *d* band, with x-ray data. Details of the density of states are deduced from the electron distributions with the aid of quantum-yield and reflectivity data by assuming (1) that direct conservation of **k** is not an important selection rule and (2) constant matrix elements. The optical conductivity and quantum yield calculated from the experimentally determined density of states are in first-order agreement with the measured values. The effects of inelastic scattering due to pair production are discussed. The contribution to the energy distribution due to single pair-production events were calculated for simple models. The results agree qualitatively with the measured energy distribution.

I. INTRODUCTION

PHOTOEMISSION may be used to study optical excitation and energy-loss processes in solids. As has been shown in previous work,[1,2] the energy distribution of photoemitted electrons provides information concerning both the absolute energy of initial and final quantum states and the selection rules for optical transitions between these states. In addition, it has been used to study scattering of excited electrons and the effect of surface conditions on electron escape. The spectral distribution of quantum yield provides information on optical excitation near the threshold and on optical absorption in quantum states below the vacuum level. Yield measurements also help in determining the cause of structure in the energy distributions which cannot be interpreted unambiguously by energy-distribution measurements alone.

Previous photoemission measurements on CdS have only been made near the threshold. Shuba[3] investigated the yield and energy distribution of photoemitted electrons from CdS between 5 and 6.5 eV on samples formed by evaporation. These samples consisted of finely dispersed hexagonal and cubic modifications of CdS. Shuba's results have been discussed by Spicer.[4] More recently, Scheer and van Laar[5] have investigated the spectral dependence of quantum yield near the threshold for CdS single crystals which were broken in air and then measured in vacuum. The results have been used to study optical transitions near the threshold and to investigate surface states. Since these measurements extended only to about 7.7 eV, they could not be used to investigate band structure over a large energy range.

Reflectivity from CdS has been measured[6] using unpolarized light up to photon energies of 25 eV for single crystals which were cleaved in air. The optical constants have been determined by a Kramers-Krönig analysis of the results on single crystals cleaved in air. Cardona[7] has studied the reflectivity to photon energies of about 9 eV. Reflection studies with polarized light[8,9] indicate a polarization dependence for some of the structure in the reflection curves.

The photoemission measurements reported here have been made to investigate band structure and energy-loss processes over as large a range of photon energies as possible. Optical-reflection and photoemission-yield data can be used in conjunction with the energy distributions to investigate the band structure below the vacuum level. The experimentally determined band structure and the assumptions concerning optical-transition probabilities can be tested by using them to calculate the optical conductivity (or imaginary part of the dielectric constant). The calculated optical conductivity can then be compared to that determined experimentally. Detailed studies have been made of the interaction of atomically clean CdS with various gases. These results will be reported elsewhere.[10]

* Work supported by the National Sciences Foundation, Washington, D. C., and by the Advanced Research Projects Agency through the Center for Materials Research at Stanford University.

† Present address: Department of Electrical Engineering, University of Colorado, Boulder, Colorado.

[1] C. N. Berglund and W. E. Spicer, Phys. Rev. **136**, A1030, A1044 (1964).

[2] E. O. Kane, Phys. Rev. **127**, 131 (1962); G. W. Gobeli and F. G. Allen, *ibid.* **127**, 141 (1962); W. E. Spicer and R. E. Simon, Phys. Rev. Letters **9**, 385 (1962); W. E. Spicer and N. B. Kindig, Solid State Commun. **2**, 13 (1964); and W. E. Spicer and C. N. Berglund, Phys. Rev. Letters **12**, 9 (1964).

[3] Iu. A. Shuba, Zh. Techn. Fiz. **26**, 1129 (1956) [English transl.: Soviet Phys.—Tech. Phys. **1**, 1103 (1956)].

[4] W. E. Spicer, J. Phys. Chem. Solids **20**, 134 (1961).

[5] J. J. Scheer and J. van Laar, Philips Res. Rept. **16**, 323 (1961).

[6] W. C. Walker and J. Osantowski, J. Phys. Chem. Solids (to be published).

[7] M. Cardona, Phys. Rev. **129**, 1068 (1963).

[8] M. Cardona, Solid State Commun. **1**, 109 (1963).

[9] W. C. Walker (unpublished).

[10] N. B. Kindig and W. E. Spicer (unpublished).

II. EXPERIMENTAL TECHNIQUES AND SAMPLES

All experiments reported here have been performed in a vacuum chamber described in detail elsewhere.[11] Clean surfaces were obtained by cleaving the samples in a pressure of less than 10^{-9} Torr provided by an 8-liter/sec VacIon pump and a titanium sublimation pump. The samples were inserted into the energy analyzer immediately after cleaving, and energy distributions and yield curves of photoemission were measured. For these experiments, monochromatic uv radiation from a McPherson Model 200 vacuum monochromator was introduced into the test chamber through a LiF window. This window established an upper limit for the measurements at about 11.8 eV.

To extend the range of measurements, the LiF window was removed from the test chamber so that the test sample surface was exposed to the 10^{-4}-Torr atmosphere of the vacuum monochromator after cleaving. In this case, the atmosphere consisted principally of H_2. The hydrogen arc then provided an essentially continuous spectrum to about 14.2 eV. Measurements were made at 16.8 and 21.2 eV by using Ne and He arcs, respectively. The results of the measurements in low vacuum were compared with the results of the measurements in high vacuum to establish the fact that the low-vacuum atmosphere did not interact with the CdS to such an extent as to obscure the bulk photoemission processes.

The energy distributions were measured by an ac method.[12] After cleaving, the first-energy distribution could be measured within three to five minutes, a time short compared to that for a monolayer of gas to strike the surface. The complete set of energy distributions could then be measured at a rate of 15 to 25 curves/h. The relative quantum yield was determined by comparing the current in the CdS photodiode with that from another photodiode which was coated with sodium salicylate[13] and which had been calibrated for absolute yield by comparison with a known standard.

Table I indicates the important characteristics of the various crystals studied in the work reported here. The high-resistance samples were illuminated with visible radiation (filtered to exclude ultraviolet) in order to make them sufficiently conducting to support the photoemission current. No difference could be detected for the semiconducting and insulating samples.

TABLE I. Description of CdS single crystals studied.[a]

Harshaw	Resistivity (Ω-cm)	Impurities
VC1	2	Pure[b]
VC2	2	Pure[b]
VC3	2	Pure[b]
VC4	10^8 (dark)	S compound
LVC1	10^8 (dark)	S compound

[a] Cleavage plane is $1\bar{2}10$.
[b] Less than 1 ppm Al, Cu, Fe, Si, Li, Na, Ca; 50 ppm Zn.

III. INTERPRETATION AND ANALYSIS OF EXPERIMENTAL DATA

A. Calculations

In previous photoemission investigations, it has been found that conservation of k may or may not be an important selection rule for optical transitions, and that photoemission may be used to investigate the importance of k conservation as a selection rule.[1,14] In cases where it is not an important selection rule, and if constant matrix elements are assumed, the energy distribution of emitted electrons is given by the equation[1]

$$N(E,h\nu)dE=\frac{T(E)S(E,h\nu)N_c(E)N_v(E-h\nu)dE}{\int_{E_G}^{h\nu}N_c(E)N_v(E-h\nu)dE}, \quad (1)$$

where N_v, N_c is the valence- and conduction-band densities of states, $T(E)$ is an escape function, E_G is the band-gap energy, $S(E,h\nu)$ is the fraction of excited electrons of energy E lost because of scattering, which is represented by

$$S(E,h\nu)=\frac{\alpha(h\nu)L(E)}{1+\alpha(h\nu)L(E)}. \quad (2)$$

In this paper, the symbol E will be used to indicate the energy of an electron in the crystal. The zero of energy will be taken at the valence-band maximum. Equation (1) gives the ratio of the number of electrons emitted with energy E in range dE to the number of electrons excited in the volume; i.e., it is a normalized energy distribution. The measured energy distribution under the above assumptions is given by

$$N_m(E,h\nu)dE=[K(h\nu)/\alpha(h\nu)]\times T(E)S(E,h\nu)N_c(E)N_v(E-h\nu)dE \quad (3)$$

in which $K(h\nu)$ is a scale factor which includes certain parameters of the experimental apparatus such as amplification factors [see Appendix A, Eq. (A12)].

In the derivation of Eqs. (1) and (2), it has been assumed that electrons are lost owing to scattering *out* of the distribution and no account has been taken of the possibility of electrons being scattered *into* the distribution from higher energies. This assumption is viable for sufficiently low photon energies. For the high-vacuum-cleaved (VC) samples, the assumption seems good for $h\nu<11$ eV. The effects of electrons being scattered into the distribution are clearly seen for higher values of $h\nu$

[11] N. B. Kindig and W. E. Spicer (unpublished).
[12] W. E. Spicer and C. N. Berglund, Rev. Sci. Instr. **35**, 1665 (1964).
[13] A. M. Smith, Ph.D. dissertation, Institute of Optics, The University of Rochester, Rochester, New York, 1961, p. 116 and references therein (unpublished).
[14] W. E. Spicer, Phys. Rev. Letters **11**, 243 (1963).

in the low-vacuum-cleaved (LVC) samples, and are discussed in Sec. VF.

The quantum yield in electrons per absorbed photon is given by

$$Y(h\nu)=\int_{E_G+E_A}^{h\nu} N(E)dE$$

$$=\frac{\int_{E_G+E_A}^{h\nu} T(E)S(E,h\nu)N_c(E)N_v(E-h\nu)dE}{\int_{E_G}^{h\nu} N_c(E)N_v(E-h\nu)dE} \quad (4)$$

in which E_A is the electron affinity.

The optical conductivity $\sigma=\omega\epsilon_2$ is determined from the relation

$$\sigma(h\nu)=\frac{C}{h\nu}\int_{E_G}^{h\nu} N_c(E)N_v(E-h\nu)dE, \quad (5)$$

where C contains the matrix elements, which will be assumed to be constant in this work, and a factor giving the absolute value of the density of states. The optical conductivity is related to the absorption coefficient by

$$\alpha=\sigma/nc\epsilon_0. \quad (6)$$

Using Eq. (5), Eq. (4) may be written as

$$Y(h\nu)=\frac{C}{h\nu\sigma(h\nu)}\int_{E_G+E_A}^{h\nu} T(E)S(E,h\nu) \times N_c(E)N_v(E-h\nu)dE. \quad (7)$$

Figure 1 illustrates the way in which the above quantities are determined if $T(E)$, $N_c(E)$, and $N_v(E-h\nu)$ are known and if $S(E,h\nu)$ is assumed constant. For the purposes of the calculation, the valence-band density-of-states function is shifted with respect to the conduction-band density-of-states function by an energy equal to the photon energy. The two functions are then multiplied giving the curve labeled N_cN_v. The area under this curve is proportional to $\omega\sigma$. The curve N_cN_v is then multiplied by $T(E)$ and $S(E,h\nu)$ (the latter term is assumed to have a value of 1 in this example) to obtain the energy distribution of electrons labeled TN_cN_v. Under the assumptions used here, the quantum yield is determined by the ratio of the area under the curve TN_cN_v to the area under the curve N_cN_v.

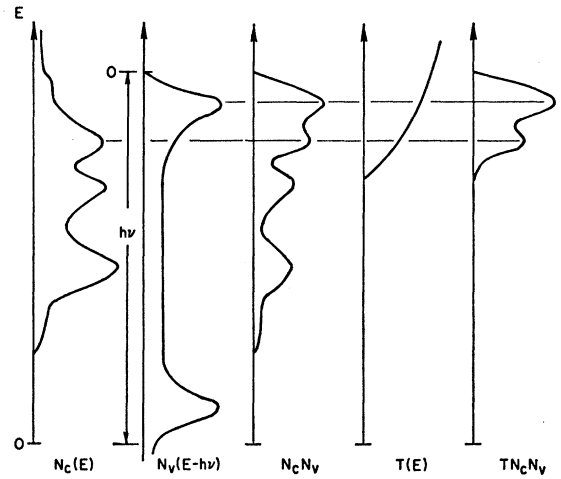

FIG. 1. Calculation of energy distributions, quantum yield, and optical conductivity using the density of states.

B. The Problem of Group Velocity

All analyses of experimental data here are based on the assumption that structure in the optical transition, probably centered at a given final energy, will produce corresponding structure in the energy distribution of the emitted electrons. For this to occur, a representative sample of the excited electrons must escape. The structure in the optical-transition probability may be associated with a critical point in the final states.[15] Since, according to band theory, $v_g=\nabla_k\mathcal{E}$ and $\nabla_k\mathcal{E}$ will be zero at the critical point in certain cases, the group velocity of these electrons will be zero. Of course, finite group velocity is a requirement for emission. This problem must be examined in detail.

It is important, first, to note that the excited electron is in a nonequilibrium state; i.e., it must lose energy through scattering processes. If the scattering is via a phonon or some other low-energy loss process, the electron may be scattered into a state with finite value of group velocity and escape from the crystal without appreciable loss of energy. In this case, information on the optical-transition probability will be retained. However, if the scattering is via pair production, the electrons will not appear in the original distribution and information concerning the optical-transition probability will be lost. A quantitative treatment of these effects will not be attempted here. However, it is clear that a peak in the distribution of emitted electrons may result from a maximum in the optical-transition probability even though the relative magnitude of this peak may be reduced. Very strong peaks in the energy distribution from silicon have been observed where the final state is a saddle point.[16] The best example is the transition to the L_3 point. A very strong maximum has been observed experimentally in the energy distributions corresponding to this transition in good agreement with calculations from band theory. In making detailed comparison between theory and experiment, Brust[17] found no evidence for a reduced escape probability for the electrons excited to the saddle point.

[15] J. C. Phillips, Phys. Rev. **125**, 1931 (1962), and references therein.

[16] W. E. Spicer and R. E. Simon, Phys. Rev. Letters **9**, 385 (1962); D. Brust, M. Cohen, and F. Bassani, *ibid.* **9**, 389 (1962).

[17] J. C. Phillips, D. Brust, and F. Bassini, Phys. Rev. Letters **9**, 389 (1962); J. C. Phillips, Phys. Rev. **133**, A452 (1964); D. Brust, *ibid.* **134**, A1337 (1964).

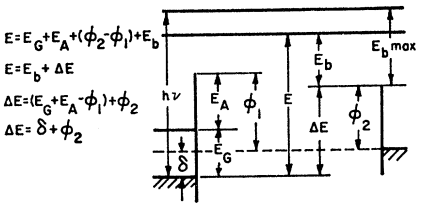

FIG. 2. Relationship for zero-retarding potential between the energy levels of an electron in vacuum E_b and in the solid E with the electron affinity, the Fermi level, and the work functions.

In the present work, some check on any distortion due to scattering may be made by the calculation of σ or ϵ_2 from the density of states determined from the photoemission studies. The curve of σ or ϵ_2 so determined can then be compared to the experimental curves. Any gross error in the determination of density of states would result in a large disagreement between calculated and measured values of σ or ϵ_2.

C. Establishment of a Reference for Electron Energy

Typical sets of energy-distribution curves for CdS cleaved in high or in low vacuum are presented in Figs. 3 through 10. The area under these curves is not normalized to yield. The applied retarding potential E_b is plotted on the abscissa and is related to the absolute energy E referred to the top of the valence band in the solid by the equation

$$E=E_b+\Delta E. \tag{8}$$

By reference to Fig. 2, it can be seen that

$$\begin{aligned}\Delta E&=E_G+E_A-(\phi_1-\phi_2),\\ \Delta E&=(E_G+E_A-\phi_1)+\phi_2=\delta+\phi_2,\end{aligned} \tag{9}$$

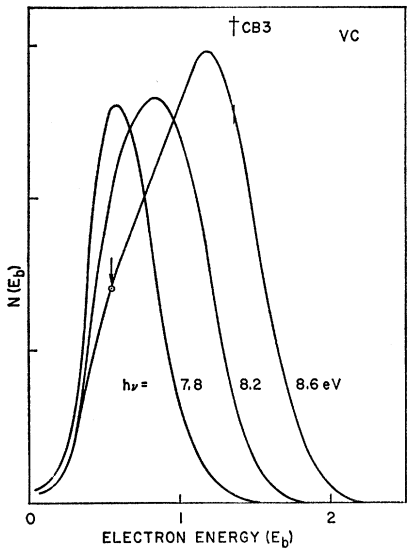

FIG. 3. Energy distributions from CdS cleaved in high vacuum. $h\nu=7.8$, 8.2, and 8.6 eV.

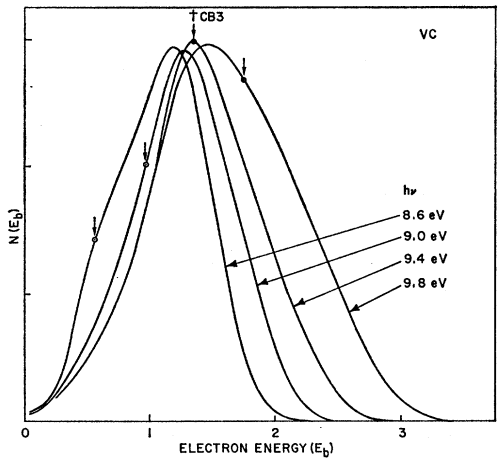

FIG. 4. Energy distributions from CdS cleaved in high vacuum. $h\nu=8.6$, 9.0, 9.4, and 9.8 eV.

where E_G, E_A, and ϕ_1 are the band gap, the electron affinity, and the work function, respectively, of the emitter, ϕ_2 is the work function of the collector, and $\delta=(E_G+E_A-\phi_1)$. In these experiments, ΔE could be obtained most accurately and directly from a measurement of the maximum value of potential $E_{b,\max}$ at which electrons appear in the energy distributions for spectral regions of relatively high yield. Assuming that the most energetic electrons come from the top of the valence band, $h\nu=E$ and

$$\Delta E=h\nu-E_{b,\max}. \tag{10}$$

For the measurements made here, ΔE could be determined only within an accuracy of ± 0.2 eV. The inaccuracy is due to variation of collector work function, excitation of carriers from states above the valence-band maximum, and the instrumentation bandwidth.

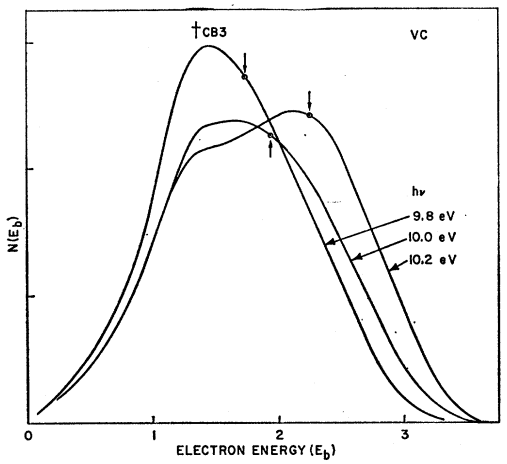

FIG. 5. Energy distributions from CdS cleaved in high vacuum. $h\nu=9.8$, 10.0, and 10.2 eV.

IV. QUALITATIVE INTERPRETATION OF EXPERIMENTAL DATA

A. Experimental Results for $h\nu \leqslant 14.2$ eV

Typical sets of energy distributions for CdS cleaved in high vacuum are presented in Figs. 3 through 6. These samples are believed to be atomically clean. Using the data in Figs. 3 through 6 and Eq. (10), a value of 6.85 ± 2 eV is obtained for ΔE. The gross features of these energy distributions can be interpreted in terms of Eq. (1) if maxima are assumed in the conduction-band density of states at $E=8.2$ eV and in the valence-band density of states at $E=-1.2$ eV. Electrons which are optically excited to the conduction-band maximum produce a peak in the energy distribution as indicated by the daggers at $E_b=1.35$ eV in Figs. 3 through 6. As predicted by Eq. (1), the position of this peak is independent of photon energy. Electrons which are optically excited from the valence-band maximum produce a peak

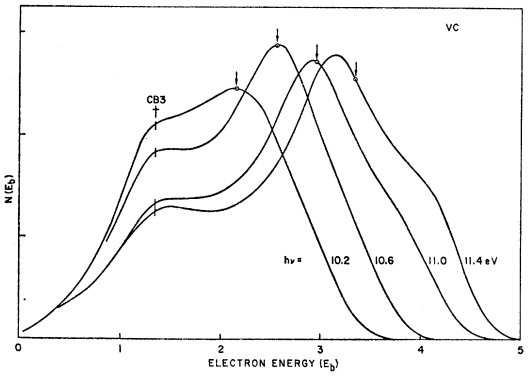

FIG. 6. Energy distributions from CdS cleaved in high vacuum. $h\nu=10.2$, 10.6, 11.0, and 11.4 eV.

which is a function of $h\nu$, its position being given by the equations

$$E_b=-8.05+h\nu \tag{11}$$

or

$$E=-1.2+h\nu. \tag{12}$$

The position of this peak as predicted from Eq. (11) is indicated by the arrows in Figs. 3 through 6.

Only for $h\nu>8.2$ eV are electrons that are excited from the maximum in the valence-band density of states able to escape in significant numbers. The "bulge" at $E_b\cong0.6$ eV in the $h\nu=8.6$ eV curve (Fig. 3) gives evidence of such escape. In the range $9<h\nu<10$ eV, the peaks due to the maxima in the conduction- and valence-band densities of states overlap, and neither of the maxima are clearly resolved; however, the detailed shapes of the energy distributions are consistent with the proposed model. For example, electrons from the maximum in the valence-band density of states which are excited to an energy below that of the maximum in the conduction-band density of states produce a "bulge" in the energy distribution. A similar "bulge" appears when

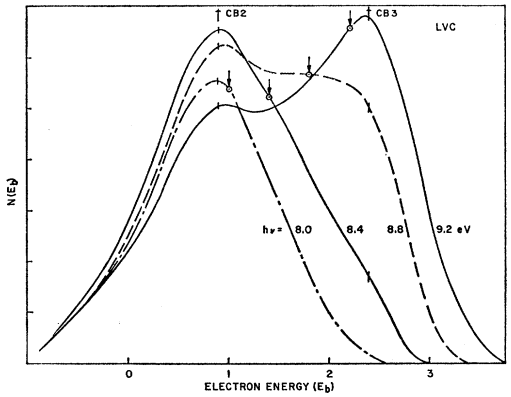

FIG. 7. Energy distributions from CdS cleaved in low vacuum. $h\nu=8.0$, 8.4, 8.8, and 9.2 eV.

electrons from the valence-band maximum are excited to states above the maximum in the conduction-band density of states. For $h\nu>10$ eV, the two maxima are well separated and easily resolved. For $h\nu>10.5$ eV, additional structure appears at high-electron energies and the peak in the energy lags slightly behind that predicted by Eq. (9). This may be due to electron-electron scattering, additional conduction- or valence-band structure, or the occurrence of direct as well as nondirect optical transitions.

Typical sets of energy distribution curves for CdS cleaved in low vacuum are given in Figs. 7 through 10 and Figs. 12 and 13. Using these data and Eq. (10), a value of 5.8 ± 0.2 eV is found for ΔE in this material.

The spectral distributions of the quantum yield are presented in Fig. 11. From these data, electron affinities of 4.8 ± 0.3 eV and 3.8 ± 0.4 eV are obtained for the VC

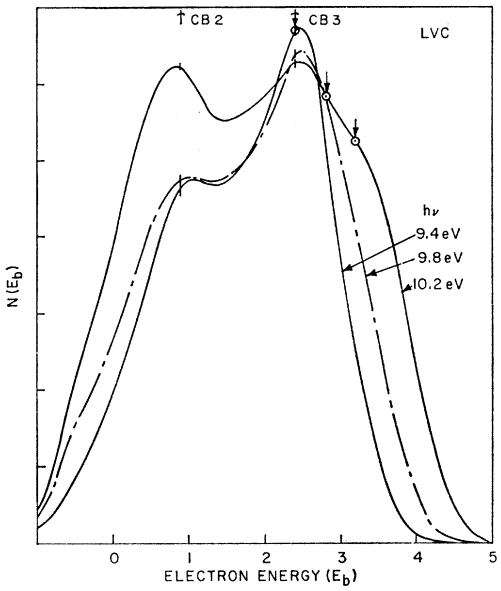

FIG. 8. Energy distributions from CdS cleaved in low vacuum. $h\nu=9.4$, 9.8, and 10.2 eV.

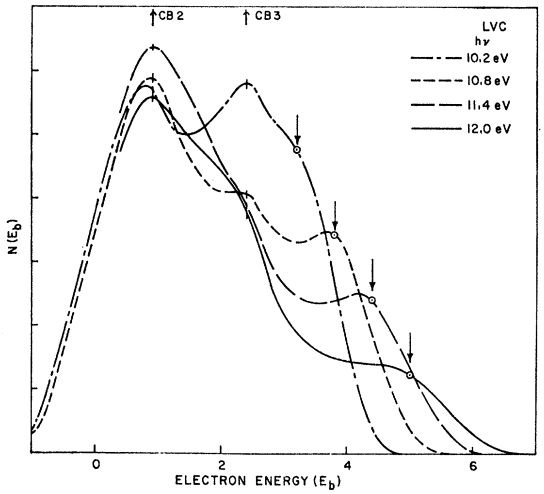

FIG. 9. Energy distributions from CdS cleaved in low vacuum. $h\nu=10.2$, 10.8, 11.4, and 12.0 eV.

and LVC samples, respectively. As a result of the lowered electron affinity of the LVC sample, it is possible to see a second maximum in the conduction-band density of states located at $E=6.7$ eV, as well as that previously located at $E=8.2$ eV in the VC sample. The positions of these peaks are indicated by daggers in the figures. The peaks associated with excitation from the valence band are indicated by arrows in the figures at

$$E_b=-7.0+h\nu, \tag{13}$$

$$E=-1.2+h\nu, \tag{14}$$

which is in agreement with the results from the sample cleaved in high vacuum. Detailed analysis has indicated that the effect of electron scattering is greater in the LVC samples than in the VC samples. This will be discussed in detail in a separate article.[10] The fact that Eqs. (11) through (14) are reasonably well satisfied over a large photon-energy range and that peaks associated with the conduction band appear at fixed energy levels

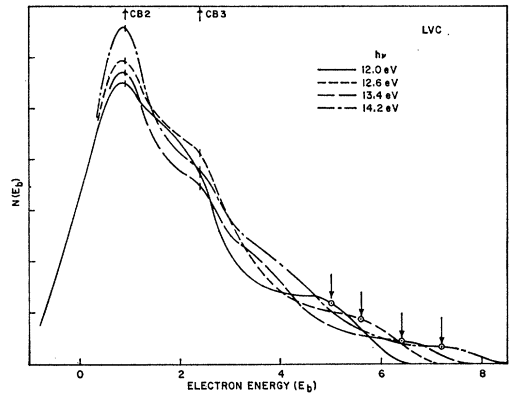

FIG. 10. Energy distributions from CdS cleaved in low vacuum. $h\nu=12.0$, 12.6, 13.4, and 14.2 eV.

in the energy distributions independent of photon energy in agreement with Eq. (1) suggests that conservation of $\mathbf{k}$ is not a dominant selection rule for the observed optical transitions in CdS.

B. Experimental Results for $h\nu \gtrsim 13$ eV

Energy distribution curves for LVC CdS for $13 \leq h\nu \leq 21.2$ eV are presented in Figs. 12 and 13. The position of maxima in the conduction-band density of states determined in the last section is again indicated by daggers, and the energy to which electrons from the maximum in the valence-band peak and d band are excited [Eqs. (13) and (15)] are indicated by arrows labeled VB and DB, respectively. The 21.2-eV curve is characterized by three strong features: the peaks at $E_b=0.8$ and at $E_b=6$ eV, and the shoulder at $E_b\cong 10$ eV. The peak at 0.8 eV is attributed to (1) excitation from the filled bands directly to the conduction-band states, (2) excited electrons which have inelastically scattered one or more times with pair production, and (3) secondary electrons excited from the filled bands by the process mentioned in (2). This peak and the small shoulder at $E_b=2.4$ eV appear at the energy of maxima in the conduction-band density of states which were identified in the last section. The shoulder at $E_b\cong 10$ eV is thought to be a result of inelastic scattering. This and the other features attributed to scattering are discussed in more detail in Sec. VF.

In this section, attention is focused on the peak at 6 eV, and data are presented which indicate that it is caused by a second maximum in the filled density of

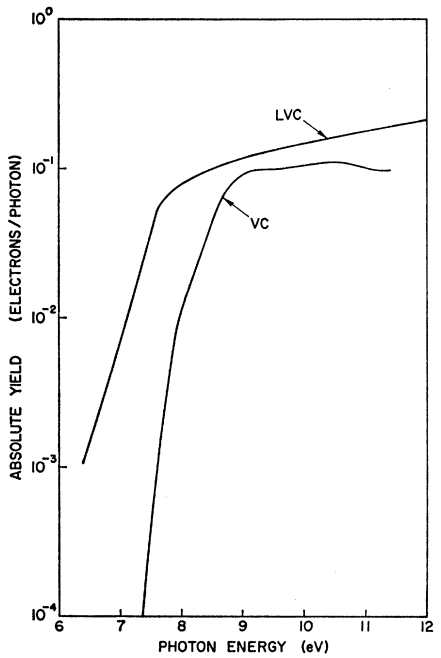

FIG. 11. Absolute quantum yield of high-vacuum cleaved and low-vacuum cleaved CdS.

states. If the peak which occurs at $E_b=6$ eV for $h\nu=21.2$ eV results from such a maximum in the filled density of states, it must satisfy the relations

$$E_b=h\nu-15.2 \text{ eV}, \quad (15)$$

$$E=h\nu-9.4 \text{ eV}, \quad (16)$$

i.e., the maximum must therefore be located at $E=-9.4$ eV. Based on optical reflectivity, it has previously been suggested[18] that the d band of Cd is located at approximately this energy in CdS. Such an assignment is also consistent with x-ray absorption measurements and atomic-energy-level diagrams.[19] As a result, the band which is located by Eq. (16) will be associated with the d shell of Cd and referred to hereafter as the d band.

This assignment of the structure in the energy distribution obtained at 21.2 eV should be confirmed by testing Eqs. (15) and (16) by measurements at other values of photon energy. Because a continuum of radiation strong enough to measure energy distributions was not available in this work for $h\nu>14.2$ eV, it was not possible to follow the movement of the d-band peak continuously. Only spectral lines of Ne at 16.8 eV and He at 21.2 eV were available. For $h\nu=16.8$ eV, electrons excited from the d band should appear at $E_b=1.6$ eV according to Eq. (15). It is apparent from Figs. 12 and 13 that the relative number of electrons near $E_b=1.6$ eV is greater for $h\nu=16.8$ eV than for either $h\nu=14.2$ or 21.2 eV. As a result of the maxima in the conduction-band density of states at 0.8 and 2.4 eV, there is a trough in the conduction-band density of states at 1.6 eV. Therefore, excitation from the d band to $E_b=1.6$ eV can be expected to produce only a shoulder in that energy range. Such a shoulder is apparent in Fig. 12.

It would be useful to obtain from the photoemission data a comparison between the number of electrons in the d band and in the valence bands. Such a comparison is difficult to obtain because of the distortion produced by electron-electron scattering; however, it is useful to compare the energy distributions for $h\nu=13$ eV and $h\nu=21.2$ eV (see Fig. 12). In the former case, electrons from the maximum in the valence-band density of states are excited to $E_b=6$ eV; in the latter case, those from the d band are excited to the same energy. It is apparent from Fig. 12 that d-band excitation is as strong or stronger than that from the maximum in the valence-band density of states. This is reasonable since there are 10 d electrons/molecule as compared to only 8 valence electrons/molecule.

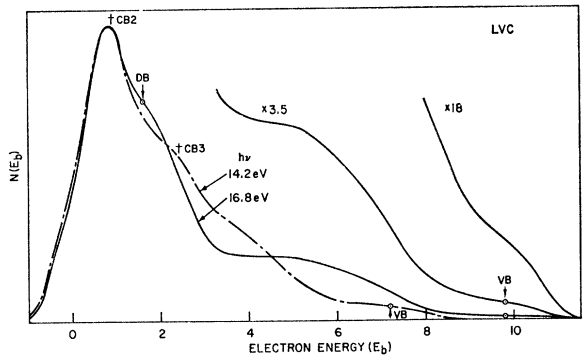

FIG. 12. Energy distributions from CdS cleaved in low vacuum. $h\nu=14.2$ and 16.8 eV.

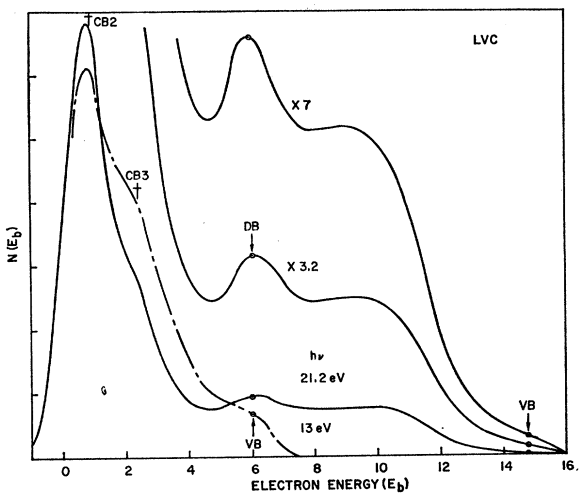

FIG. 13. Energy distributions from CdS cleaved in low vacuum. $h\nu=13.0$ and 21.2 eV.

V. QUANTITATIVE EXPLANATION OF THE EXPERIMENTAL DATA

In the previous section, maxima were located in the conduction-band density of states at $E=6.7$ and 8.2 eV and in the valence-band density of states at $E=1.2$ eV. In addition, the Cd d band was located at $E=-9.4$ eV. This section presents the following:

(1) An analysis of structure in the conduction-band density of states located below the vacuum level.

(2) A quantitative determination of the density of states of CdS.

(3) A calculation of the optical conductivity $\sigma=\omega\epsilon_2$ (ϵ_2 is the imaginary part of the dielectric constant), using the density of states determined in (2).

A. Conduction-Band Structure Below the Vacuum Level

Any conduction-band structure which lies below the vacuum level can be detected only through a study of the optical constants [Eq. (4)] and/or the quantum yield [Eq. (3)]. The optical reflectivity curves of Walker and Osantowski[6] and of Cardona[7] are shown in Fig. 14. Based on the analysis given here, reflectivity peaks would be expected when maxima in the conduction- and valence-band densities of states are separated by the

[18] M. Cardona, Bull. Am. Phys. Soc. 8, 246 (1963).
[19] R. W. Hill, E. L. Church, and J. W. Mihelich, Rev. Sci. Instr. 23, 523 (1962).

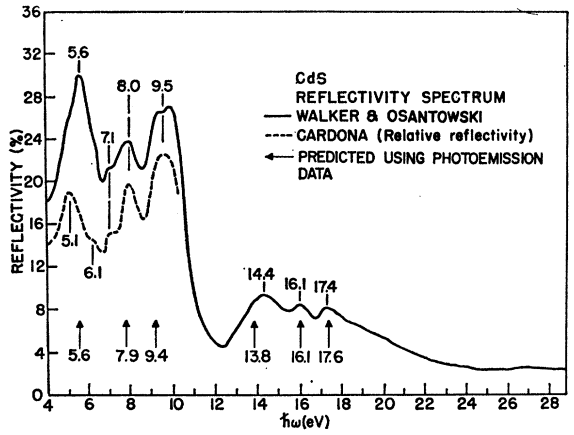

FIG. 14. Reflectivity spectra of CdS. The arrows indicate peak locations predicted using photoemission data.

photon energy. Using the density-of-states maxima identified in the last section, reflectivity peaks would be predicted at photon energies of 7.9 and 9.4 eV due to excitation from the valence-band maximum and at 16.1 and 17.2 eV due to excitation from the d band. As can be seen from Fig. 14, the four predicted peak positions are in reasonable agreement with four of the six major experimental peaks. It is suggested that the experimental peaks at 5.6 and 14.4 eV are due to transitions from the valence and d-band maxima, respectively, to a conduction-band maximum located at $E=4.4$ eV. On this model, peaks would be predicted at 5.6 and 13.8 eV in reasonable agreement with the reflectivity data.

Further evidence of this assignment is obtained from the yield curve of the LVC sample shown in Fig. 15. The denominator of Eq. (4) can be separated into two terms[20]; i.e., α_a represents absorption above the vacuum level and α_b represents absorption below the vacuum level. The yield can then be written as

$$Y \propto \alpha_a/(\alpha_a+\alpha_b) \tag{17}$$

if scattering is neglected. According to Eqs. (4) and (17), a minimum should appear in the yield when a maximum occurs in the absorption coefficient to states below the vacuum level. Such a minimum should occur when the photon energy is equal to the difference between the d band and the lowest maximum in the valence-band density of states, i.e., at about $h\nu=14$ eV. As can be seen from Fig. 15, the yield falls steeply in just this region.

B. Determination of the Conduction- and Valence-Band Densities of States

By making use of both photoemission and optical data and certain assumptions, it is possible to determine the relative density of states in the conduction, valence, and d bands. A large amount of information can be obtained directly from the energy-distribution curves. If the assumptions on which it is based hold, Eq. (3) can be used directly to determine one density of states[21] if the other is constant over a large energy range.[14] If considerable structure exists in both the conduction- and valence-band densities of states, Eq. (3) can still be used to determine the valence-band density of states for states well above the vacuum level. The method is described in detail in Appendix B. As shown there, a density of states $N_v'(E)$ is first obtained which differs from the real density of states by a factor of $\exp(-aE)$.

$$N_v'(E)=N_v(E)\exp(-aE). \tag{18}$$

The parameter a is a constant which is determined by the use of measured quantum yield as will be discussed below.

The conduction-band density of states is given by

$$M_c'(E)=M_c(E)\exp\{a[E-(E_G+E_A)]\}. \tag{19}$$

The term

$$M_c(E)=T(E)S(E)N_c(E-h\nu) \tag{20}$$

can be determined if S is not a function of photon energy. If independent means for determining $T(E)$ and $S(E)$ are not available, N_c can only be determined accurately in a limited energy range. The electron energy must be far enough above the threshold for escape and below the threshold for scattering so that the factors T and S can be treated as constant.

The energy distributions $N_M(E)$ determined from the calculated densities of states are given by

$$N_M(E)\propto N_c'(E)N_v'(E-h\nu)$$
$$=N_c(E)N_v(E-h\nu)\exp\{a[h\nu-(E_G+E_A)]\} \tag{21}$$

and differ from the actual energy distributions by the factor $\exp\{a[h\nu(E_G+E_A)]\}$. This factor adjusts the amplitude of the curves but does not affect the shape.

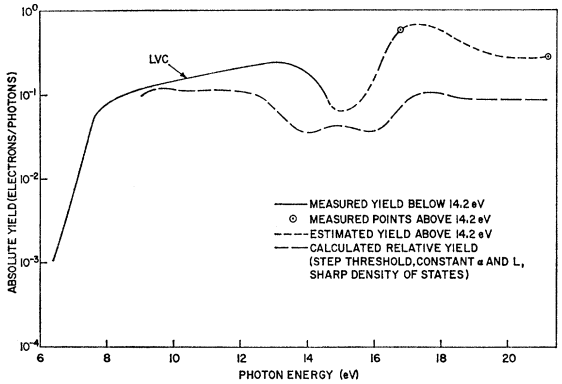

FIG. 15. The measured absolute quantum yield for low-vacuum cleaved CdS and the yield calculated, neglecting the effects of scattering.

[20] W. E. Spicer, J. Appl. Phys. 31, 2077 (1960); W. E. Spicer, Proc. IEEE 51, 1119 (1963); and W. E. Spicer, Phys. Rev. 112, 114 (1958).

[21] J. Bardeen, F. J. Blatt, and L. H. Hall, *Photoconductivity Conference*, edited by R. G. Breckenridge (John Wiley & Sons, Inc., New York, 1956), p. 146.

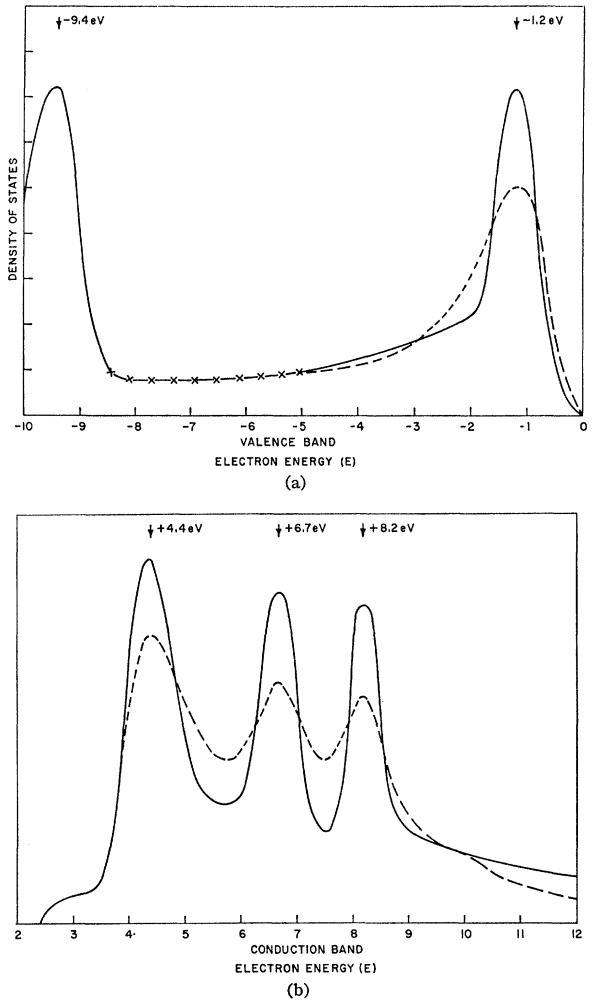

FIG. 16. The density of states of CdS determined from photoemission data.

It is determined by normalizing the calculated yield to the measured quantum yield (using the measured optical conductivity) at widely separated photon energies in order to minimize errors due to uncertainty in the conductivity or the yield. The calculated yield $Y'(h\nu)$ from Eqs. (6) and (7) is

$$Y'(h\nu)=C\int_{E_G+E_A}^{h\nu} M_c'(E)N_v'(E-h\nu)dE \Big/ h\nu\sigma(h\nu). \quad (22)$$

The parameter a is adjusted by trial and error so that $Y'(h\nu_B)/Y'(h\nu_A)=Y(h\nu_B)/Y(h\nu_A)$. The portion of the valence-band density of states in Fig. 16 above $E=-5$ eV was obtained by the method described here.

It was apparent from the energy distributions that there was no density-of-states structure in the range -8.4 eV$\leq E\leq -5$ eV. Because of the effect of scattered electrons, it was only possible to put an upper limit on the density of states in this energy range. This limit is indicated in Fig. 16. The accuracy between $E=-3.5$ eV and $E=-5$ eV is not high. It is possible that $N(E)$ goes gradually to zero over this energy range. The shape of the d-band density of states was obtained directly from the 21.2-eV energy distribution curve; however, only a rough estimate of the magnitude of this peak could be obtained from the energy distributions. As a result, the magnitude of this peak was determined principally from calculation of σ and comparison of it with the experimental value.

The quantity $M(E,h\nu)=T(E)S(E,h\nu)N_c(E)$ is determined by assuming that $T(E)$ is approximately constant for values of E sufficiently greater than (E_G+E_A). By making use of this fact and by assuming that $S(E,h\nu)$ was constant, the conduction-band density of states was estimated in the range $8.6\leq E\leq 11.6$ eV from the sample cleaved in high vacuum. In the energy range $6\leq E\leq 9$ eV, the density of states was estimated from the energy distribution of CdS cleaved in low vacuum (Figs. 7 through 10).

In Fig. 16, two densities of states are shown for $E>-5$ eV, the dashed curve is that obtained directly from the considerations discussed above. The other curve was sharpened to give better agreement between the calculated and measured values of σ. Such a sharpening is necessary since the measured energy distributions will be broadened as a result of (1) energy loss due to lattice scattering, (2) any small band bending which may be present, and (3) instrumentation bandwidth, and (4) the group-velocity problem discussed in IIB.

C. Calculation of the Quantum Yield

As mentioned above, a calculation of quantum yield was used as an aid in determining some features of the

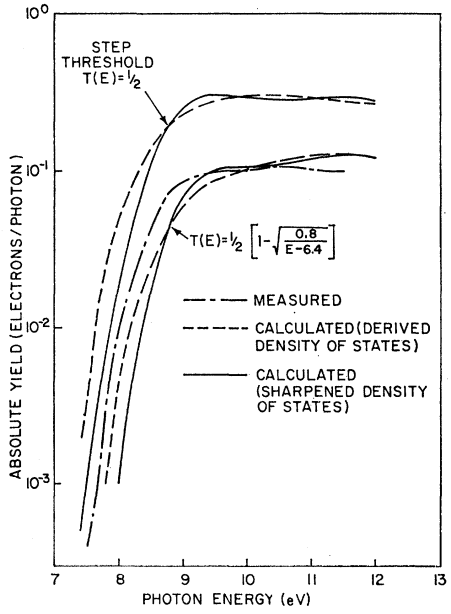

FIG. 17. Comparison of the measured and calculated yield for CdS.

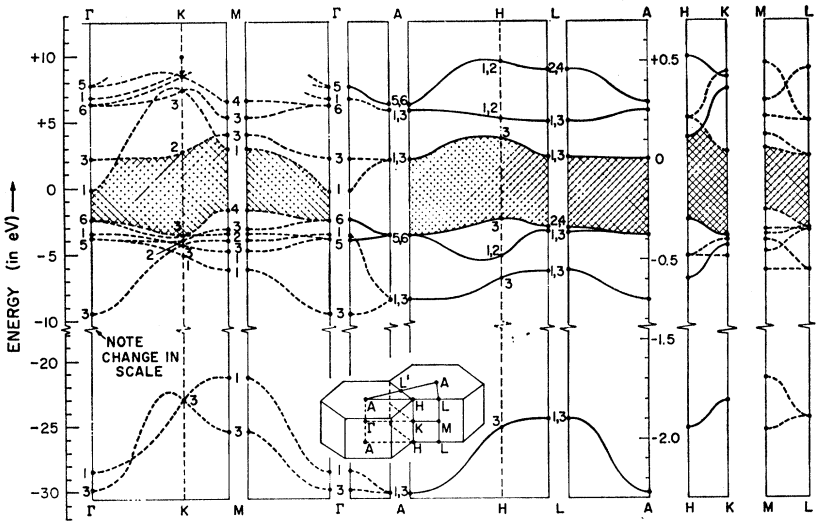

FIG. 18. The calculated band structure of ZnS (Herman and Skillman). The calculated band structure of CdS is very similar (Ref. 27).

density of states. The quantum yields calculated for $h\nu \leq 12$ eV using both the original and the sharpened densities of states and Eq. (4) are shown in Fig. 17.

In this calculation, the scattering term $S(E)$ is assumed to be constant and to have unity value. The escape (threshold) function is assumed to be either a step function with a value of $\frac{1}{2}$ or an energy-dependent function given by[22]

$$\begin{aligned} T(E)&=\tfrac{1}{2}\{1-[0.8/(E-6.4)]^{1/2}\} \quad \text{for } E>7.2 \text{ eV}, \\ T(E)&=0 \qquad\qquad\qquad\qquad\quad \text{for } E<7.2 \text{ eV}. \end{aligned} \tag{23}$$

The energy associated with the critical momentum for escape is arbitrarily assumed to be 0.8 eV. This low value is chosen because photoemission near the threshold is expected to occur from relatively narrow bands as can be seen from the calculated band structure in Fig. 18. The effect of elastic scattering may make the threshold function rise more rapidly than predicted by an equation of the form of Eq. (23). A step threshold function should set the upper limit of the escape probability. As can be seen from Fig. 17, the use of a step threshold produces a curve which has almost the same shape as the experimental curve. However, the resulting absolute yield is too large by a factor of 3 at high photon energies. The energy-dependent threshold function gives the correct yield at high photon energies, but gives too low a yield in the threshold region. The experimentally observed structure at about 9.4 eV is somewhat more apparent in the calculated curves if the sharpened density of states is used.

Crude estimates may be placed on the limits of the attenuation L for $6.5<E<11.5$ eV using the data given above. A value of $S(E,h\nu)$ of $\frac{1}{3}$ [see Eq. (2)] must be used to bring the experimental and calculated yield curves into agreement if the step threshold $[T(E)=\frac{1}{2}]$ is used in Eq. (4). Using $\alpha=7.7\times10^5$/cm, a lower limit of 65 Å is obtained for L. If Eq. (23) is used for $T(E)$, $L\gg130$ Å.

The principal features of the experimental yield curve for $9<h\nu<21.2$ eV may be predicted by use of the expression

$$Y \propto \alpha_a/(\alpha_a+\alpha_b). \tag{17}$$

In Eq. (23), only the ratio of the probability of electron excitation to states above the vacuum level (proportional to α_a) to the total probability for excitation [proportional to $(\alpha_a+\alpha_b)$] is considered. No consideration is made of the effects of electron scattering. Using Eqs. (3) and (4) and assuming constant matrix elements, Eq. (17) reduces to

$$Y(h\nu) \propto \frac{\int_{E_G+E_A}^{h\nu} N_c(E)N_v(E-h\nu)dE}{\int_{E_G}^{h\nu} N_c(E)N_v(E-h\nu)dE}. \tag{24}$$

Using the sharpened densities of states determined previously and Eq. (24), the yield curve shown in Fig. 15 was calculated. The absolute value of the calculated yield curve has been set arbitrarily. As mentioned previously, the general features of the experimental curve are given by this crude model. It should be noted that the relative drop in the calculated yield near 15 eV and the rise near 17 eV are both smaller in the calculated curve than in the experimental one. This is probably due to the neglect of the effects of electron-electron scattering (i.e., pair production) in the calculation. Neither the loss of electrons at 15 eV due to scattering states below the vacuum level nor the addition of secondary electrons at higher photon energies has been taken into account in the calculation.

[22] R. H. Fowler, Phys. Rev. 38, 45 (1931).

D. Calculation of the Optical Conductivity

The optical conductivity has been calculated using Eq. (5) for both the derived and the sharpened densities of states. The results are shown in Fig. 19. The general agreement between the calculated and the measured optical conductivities[23] indicates the correctness of the gross features of the density of states and of the assumption of nondirect transitions and constant matrix elements. Lack of detailed agreement can be attributed to either the lack of resolution in the photoemission experiments or the partial breakdown of the assumptions on which the calculations are based, i.e., to the variation in matrix elements and to the contribution of direct transitions.

E. The Calculated Band Structure of CdS

The band structures of CdS and ZnS have been calculated by Herman and Skillman[24] who used an OPW method without considering spin-orbit splitting. The results for ZnS are shown in Fig. 18. (The CdS results were so similar that they were not published.[25]) The features of the band structure found in this work are in general agreement with the calculated band structure. In particular, the rather surprisingly flat, high-density conduction bands lying well above the conduction-band minimum predicted by the theory were found in this work. The calculations indicate strong structure in the density of states with maxima located approximately 2, 6, and 10 eV above the conduction-band minimum and the narrow valence bands with a maximum density of states occurring about 2 eV below the valence-band edge. These results are in general agreement with the results reported here.

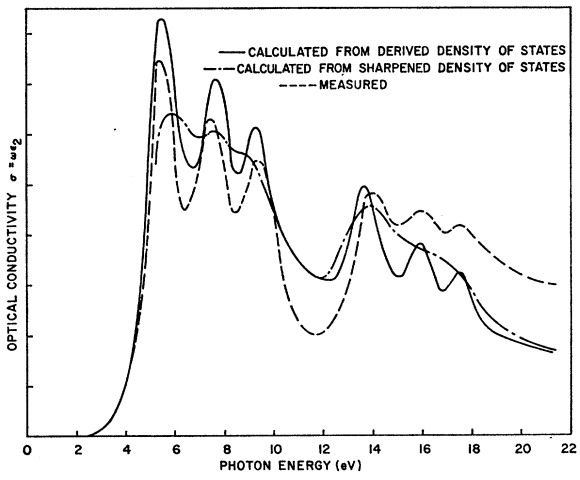

FIG. 19. Comparison of the measured and calculated optical conductivity σ of CdS. The solid curve is determined from the derived density of states. The dash-dot curve is determined from the sharpened density of states.

F. The Effects of Scattering

1. Experimental Data

Several effects due to scattering by pair-production events can be seen particularly well in the LVC energy distribution curves (Figs. 7 through 10 and Figs. 12 and 13) since data for these samples could be taken over a large range of photon energies. A peak or shoulder occurs at the high-energy end of the distribution due to electrons excited from the valence-band maximum at $E=-1.2$ eV. As the photon energy increases, this peak steadily diminishes in size and gradually changes from a peak to a shoulder due to the increase probability of scattering via pair production as electron energy is increased. The scattered electrons (both primaries and secondaries) appear at low energies. This adds to emission near the conduction band maxima at $E_b=0.9$ and 2.4 eV due to multipli-scattered electrons, and produces a new shoulder in the energy distribution at about 5 eV less than the maximum energy (see Figs. 12 and 13) due to once-scattered electrons. In the following paragraphs the loss of high-energy electrons due to scattering and the energy distribution of once-scattered electrons are discussed in more detail.

2. The Loss of High-Energy Electrons Due to Scattering

The loss of high-energy electrons in the energy distribution is estimated by using the following equation[26]:

$$S(E,h\nu)=\frac{\alpha(h\nu)L(E)}{1+\alpha(h\nu)L(E)}. \tag{2}$$

The attenuation length $L(E)$ depends on both the elastic $l_p(E)$ and the inelastic $l_e(E)$ scattering mean free paths. These quantities have been related by Monte Carlo calculations[27] and by age theory.[28] Here, l_p can be considered to be independent of energy, whereas $l_e(E)$ will be infinite for values of energy less than the threshold energy for pair production. For energy greater than the threshold, $l_e(E)$ will decrease rapidly with increasing energy.[26]

At small values of E, $L(E)\gg 1/\alpha(h\nu)$. In this limit, $S(E)$ goes to unity. As E increases, $L(E)$ will decrease. In the limit of $L(E)\ll 1/\alpha(h\nu)$, $S(E)$ approaches $L(E)\alpha(h\nu)$ (a quantity much smaller than unity) as a limit. Thus, as the electron energy of the excited electrons increases, the number of electrons which escape without inelastic scattering can be expected to decrease. As discussed in Sec. F1, this is observed experimentally.

An estimate of the energy dependence of l_e can be

[23] W. C. Walker and J. Osantowski (private communication).
[24] F. Herman and S. Skillman, *Proceedings of the International Conference on Semiconductor Physics, Prague, 1960* (Academic Press Inc., New York, 1961), p. 20.
[25] F. Herman (private communication).
[26] W. E. Spicer, J. Phys. Chem. Solids **22**, 365 (1961).
[27] R. Stuart, F. Wooten, and W. E. Spicer, Phys. Rev. **135**, A495 (1964).
[28] S. M. Sze and J. L. Moll (to be published).

made by taking the reciprocal of the inelastic scattering probability per unit time[1] $P_s(E')$ derived on a density-of-states argument in Appendix C.

3. *The Energy Distribution Due to Electrons Involved in a Single Pair-Production Event*

For photon energies considerably larger than the band gap, electrons involved in pair-production events may have sufficient energy to escape from the solid and to appear in the energy distributions.[26] The energy distribution of these electrons may provide useful information about the relationship between the band structure and the scattering process.

Berglund and Spicer[1] have developed an approximate treatment for the energy distribution of once-scattered electrons. In Appendix C this treatment is examined and placed in a form best suited for this work. The mathematical treatment of electrons scattered by multiple pair production events is much more difficult and will not be attempted here. Equation (C3) of Appendix C gives the energy distribution, including the once-scattered contribution. The second term in the brackets of Eq. (C3) is reproduced here as Eq. (25). This can be used to make an estimate of the energy distribution of once-scattered electrons in the solid.

$$g(E)=2\int_E^{h\nu}\frac{p_s(E',E)}{P_s(E')}\alpha'(E')dE'. \qquad (25)$$

Using Eq. (C2) and the density of states shown in Fig. 16, $P_s(E')$ has been calculated. The results of this calculation are presented in Fig. 20. Several approximations have been made in order to use Eq. (25) to calculate the scattering in CdS at photon energies of 16.8 and 21.2 eV:

(1) Optical excitation occurs from the valence-band peak to the final conduction-band energies between about 14 and 21.2 eV where the conduction-band density of states is nearly constant. Therefore, $\alpha'(E')$ is proportional to $N_v(E'-h\nu)$.

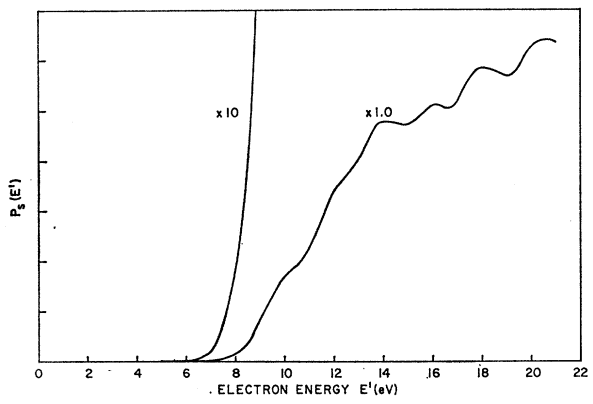

FIG. 20. The integrated scattering probability for CdS.

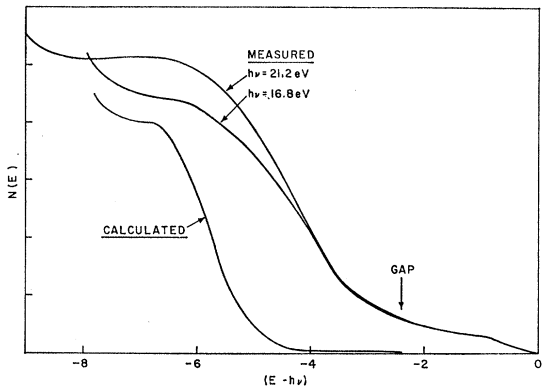

FIG. 21. Measured energy distributions at 16.8 and 21.2 eV compared with the calculated energy distribution of once-scattered electrons.

(2) $P_s(E')$ is approximately constant over the same range of final energies, as can be seen in Fig. 20.

(3) The conduction-band density of states $N_c(E)$ is assumed to be constant over the range of final energies E to which electrons can scatter from E'. As can be seen from Fig. 16, this is a reasonable assumption.

Using the above assumptions, Eq. (25) can be written as

$$g(E)\propto\int_E^{h\nu}N_v(E'-h\nu)\times\int_0^{\infty}N_v(E_0)N_c(E_0+E'-E)dE_0dE' \qquad (26a)$$

or, using Eq. (5),

$$g(E)\propto\int_E^{h\nu}[N_v(E'-h\nu)](E'-E)[\sigma(E'-E)]dE'. \qquad (26b)$$

Energy distributions of once-scattered electrons calculated using Eq. (26b) are compared in Fig. 21 with the measured energy distributions. The electron energy referred to the maximum possible energy (i.e., $E-h\nu$) is plotted as the abscissa. A shoulder in the experimental curves at about -6.5 eV is qualitatively predicted by the calculation. The number of electrons losing an energy just larger than the band gap in the measured curve is much larger than predicted by the theory.

Other evidence appears in the energy distributions to indicate that a measurable number of electrons lose an amount of energy just larger than the band gap. This can be seen by comparing the ratio of the magnitude of the peak at $E_b=0.9$ eV ($E=6.7$ eV) to that of the peak at $E_b=2.4$ eV ($E=8.2$ eV) in the LVC energy distributions for $h\nu>10$ eV as shown in Fig. 22. In this range of photon energy, scattered electrons provide a large fraction of the electrons escaping at these energies. The ratio increases for increasing photon energies up to $h\nu=11.2$ eV. Then it dips through a rather sharp mini-

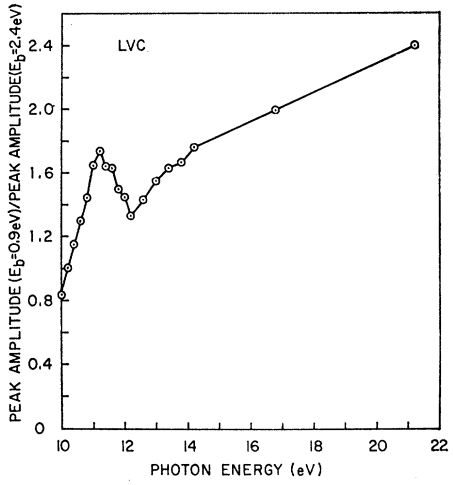

FIG. 22. The ratio of peak heights at $E_b=0.9$ and 2.4 eV in the energy distributions for CdS cleaved in low vacuum.

mum at $h\nu=12.2$ eV. From 14.0 to 21.2 eV, it continues to rise gradually. The minimum ratio should occur when the relative probability of scattering to $E=8.2$ eV passes through a maximum. The fact that this occurs when the peak in the initial distribution is at $E=11$ eV indicates that a maximum in the energy distribution of scattered electrons occurs in this photon energy range for an energy loss of about 2.8 eV.

In conclusion, the above calculations give possible explanations of features appearing in the energy distributions due to once-scattered electrons. The failure to include multiple-scattered electrons, the lack of detailed knowledge of the density of states at high energies, and the assumptions of constant matrix elements and nondirect transitions would be expected to contribute to the absence of detailed agreement.

VI. CONCLUSIONS

Photoemission measurements have been used to determine important features of the band structure of CdS. An estimate of the density of states has been obtained from 10 eV below the valence-band maximum to 12 eV above that point. Four maxima in the density of states have been detected directly by means of the energy distribution of photoelectrons. Maxima occur at -1.2 ± 0.3 eV and at -9.4 ± 0.5 eV, where the zero of energy is taken as the valence-band maximum. The former is the maximum in the valence-band density of states whereas the latter is associated with the d levels of Cd. Two maxima in the conduction-band density of states are located at 6.7 ± 0.3 eV and at 8.2 ± 0.3 eV above the top of the valence band.

A third maximum in the conduction-band density of states has been located at 4.4 ± 0.5 eV above the top of the valence band by the combined use of reflection and photoemission-yield data. The structure in the valence- and conduction-band densities of states is in general agreement with the band structure calculated by Herman and Skillman.[24]

First-order agreement is obtained between (1) optical conductivity calculated from the derived density of states, assuming that conservation of $\mathbf{k}$ is not an important selection rule and that matrix elements are independent of energy, and (2) optical conductivity determined experimentally by Walker and Osantowski[23] from reflection measurements. This agreement provides an independent check on the determination of band structure and optical selection rules. The yield calculated from the density of states is also in first-order agreement with the measured yield.

Because of the assumptions involved in their determination, the density of states determined here can only be considered a first approximation. However, the general agreement between the features of σ and yield calculated using the density of states and those measured experimentally suggests that it is a good first approximation.

The data reported here indicate that k conservation is not an important selection rule for many transitions in CdS. Similar behavior has been reported in other materials.[1,14]

It is difficult to distinguish between direct and nondirect transitions if narrow bands exist in both the valence and conduction bands as they do for CdS. It would be completely impossible to distinguish between direct and nondirect transitions if the widths of the bands were smaller than the resolution of the instrumentation. However, the resolution of the instrumentation used here is believed to be 0.1 to 0.2 eV,[12] whereas the minimum measured bandwidths are approximately 1 eV. Thus, the fact that the experimental evidence indicates that a majority of transitions are nondirect is significant. This conclusion is supported by the first-order agreement between the measured and calculated values of the optical conductivity σ and the quantum yield. However, there are two features of the experimental data which have not yet been explained in this work. The first of these features is the behavior of the peak associated with the valence-band maximum for $11<h\nu<11.6$ eV for the VC sample (see Fig. 6). This behavior may be due to electron-electron scattering, additional conduction- or valence-band structure, or the occurrence of direct as well as nondirect optical transitions. The other feature is the fact that, whereas the nondirect model explains the gross features of the optical absorption, other structure is found experimentally which is not predicted on the model used here. On the basis of this evidence, there is the possibility that direct as well as nondirect transitions are important in CdS.

The experimental techniques and equipment developed are being used to perform photoemission measurements on many other II–VI compounds. A continued systematic study of the cubic and hexagonal crystals in this class of compounds is necessary to determine the

role played by crystal symmetry as compared with that played by the constituent atoms in determining the band structure of the compounds. It should also throw additional light on the question of direct and nondirect transitions.

ACKNOWLEDGMENTS

The authors would like to express their appreciation to C. N. Berglund, F. Herman, and W. Walker for many stimulating conversations. They are grateful to W. Walker and J. Osantowski for access to unpublished data. They would also like to express their appreciation to P. McKernan and N. Andrews for work on the phototubes and sample chambers.

APPENDIX A: DERIVATION OF EXPRESSIONS FOR YIELD AND ENERGY DISTRIBUTIONS

The energy distribution of photoemitted electrons as derived by Berglund and Spicer[1] under the assumption that there are no electrons scattered *into* the energy distribution is given by

$$N(E,h\nu)dE=T(E)\frac{\alpha'(E,h\nu)}{\alpha(h\nu)}\frac{1}{1+[1/\alpha(h\nu)L(E)]}dE, \quad \text{(A1)}$$

where $T(E)$ is the escape function, $\alpha'(E,h\nu)$ is the absorption per unit of electron-energy range, $\alpha(h\nu)$ is the absorption coefficient, and $L(E)$ is the attenuation length. The absorption coefficient is related to the optical transition probability per unit time N_T by the equation

$$\alpha'(E,h\nu)=(2h\nu/\eta c\epsilon_0\mathcal{E}_0^2)N_T(E,E_0,h\nu), \quad \text{(A2)}$$

in which η is the index of refraction and $\mathcal{E}_0$ is the electric field strength. E_0 and E are, respectively, the initial and final energies of the electron. The absorption coefficients α and α' are related by

$$\alpha(h\nu)=\int_{E_G}^{h\nu}\alpha'(E,h\nu)dE, \quad \text{(A3)}$$

where E_G is the band-gap energy. For nondirect transitions,[1] the transition probability per unit time per unit energy is given by

$$N_T(E,E_0,h\nu)dE=f\mathcal{E}_0^2N_c(E)N_v(E-h\nu)dE \quad \text{(A4)}$$

in which the oscillator strength f is assumed to be independent of E. The conduction- and valence-band densities of states are N_c and N_v, respectively. Substitution of Eqs. (A2) through (A4) in Eq. (A1) yields the relation

$$N(E,h\nu)dE=\frac{T(E)N_c(E)N_v(E-h\nu)S(E,h\nu)dE}{\int_{E_G}^{h\nu}N_c(E)N_v(E-h\nu)dE} \quad (1)$$

in which $S(E,h\nu)=\alpha(h\nu)L(E)/1+\alpha(h\nu)L(E)$ is the scattering term. The quantum yield is obtained by integrating Eq. (A1) or (1) over E

$$Y(h\nu)=\int_{E_G+E_A}^{h\nu}N(E,h\nu)dE \quad \text{(A5)}$$

$$=\int_{E_G+E_A}^{h\nu}T(E)\alpha'(E,h\nu)S(E,h\nu)dE\Big/\alpha(h\nu) \quad \text{(A6)}$$

$$=\frac{\int_{E_G+E_A}^{h\nu}T(E)S(E,h\nu)N_c(E)N_v(E-h\nu)dE}{\int_{E_G}^{h\nu}N_c(E)N_v(E-h\nu)dE}. \quad \text{(A7)}$$

The measured energy-distribution curves are given by

$$N_M(E,h\nu)dE=K_1(h\nu)N(E,h\nu)dE, \quad \text{(A8)}$$

where K_1 is a scale factor which depends on the gain of the amplifiers and the intensity of the light source. The area under the measured energy-distribution curve is

$$\int_{E_G+E_A}^{h\nu}N_M(E,h\nu)dE=K_1(h\nu)\int_{E_G+E_A}^{h\nu}N(E,h\nu)dE. \quad \text{(A9)}$$

Division of Eq. (A9) by yield shows the effect of normalizing the energy distribution to yield since

$$K_1(h\nu)=\frac{\int_{E_G+E_A}^{h\nu}N_M(E,h\nu)dE}{Y(h\nu)}=\frac{\text{measured area }(h\nu)}{Y(h\nu)}. \quad \text{(A10)}$$

It is also useful to rewrite Eq. (A7) using Eqs. (A1) and (A2) in the form

$$N_M(E)dE=\frac{K_1(h\nu)}{\alpha(h\nu)}\frac{2h\nu f}{\eta c\epsilon_0}T(E)S(E,h\nu)\times N_c(E)N_v(E-h\nu)dE. \quad \text{(A11)}$$

A quantity K which is a function of $h\nu$ but not of E is then defined as

$$K=K_1(h\nu)2h\nu f/\eta c\epsilon_0. \quad \text{(A12)}$$

APPENDIX B: DETERMINATION OF DENSITY OF STATES FROM ENERGY-DISTRIBUTION CURVES

Figure 23 shows the relationship between two energy distribution curves at photon energies $h\nu_A$ and $h\nu_B$ and the density of states. Hereafter, the subscripts A, B, etc., are used to represent photon energies; the subscripts c_1, c_2, etc., conduction-band energies; and the subscripts v_1, v_2, etc., valence or d-band energies. The amplitude of the measured energy-distribution curve is designated by the photon energy and the conduction-

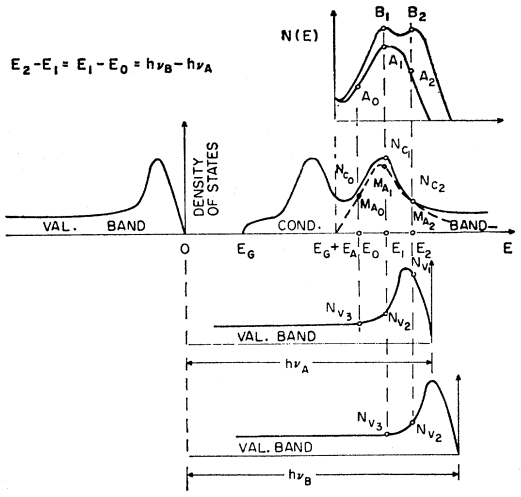

FIG. 23. Diagram illustrating calculation of the energy distributions from the density of states.

band energy, A_1, A_2, etc., where A_1 indicates the energy distribution at a conduction-band energy c_1 excited by photons of energy A. The amplitudes of the two energy distribution curves in Fig. 23 at energies E_0, E_1, and E_2 which are separated by an energy $h\nu_B-h\nu_A$ can be written as

$$A_0=(K_A/\alpha_A)M_{A_0}N_{v_3}, \tag{B1a}$$

$$A_1=(K_A/\alpha_A)M_{A_1}N_{v_2}, \tag{B1b}$$

$$A_2=(K_A/\alpha_A)M_{A_2}N_{v_1}, \tag{B1c}$$

$$B_1=(K_B/\alpha_B)M_{B_1}N_{v_3}, \tag{B1d}$$

$$B_2=(K_B/\alpha_B)M_{B_2}N_{v_2}, \tag{B1e}$$

in which K_A and K_B are used for the symbols $K(h\nu_A)$ and $K(h\nu_B)$ [see Eq. (3)], respectively, and

$$M_{A_0}=\frac{T(E_0)N_c(E_0)}{1+1/\alpha(h\nu_A)L(E_0)},$$

etc. If the energy distributions are assumed to be given by the above equations, the relative magnitude of the entire valence-band density of states can be found within an exponential multiplier using one pair of energy-distribution curves if $\alpha(h\nu)$ is known. Implicit in these equations is the assumption that appreciable numbers of electrons are not scattered into the distribution. The ratios B_2/A_2 and B_1/A_1 are now given by

$$\frac{B_2}{A_2}=\left(\frac{K_B/\alpha_B}{K_A/\alpha_A}\right)\left(\frac{N_{v_2}}{N_{v_1}}\right), \tag{B2}$$

$$\frac{B_1}{A_1}=\left(\frac{K_B/\alpha_B}{K_A/\alpha_A}\right)\left(\frac{N_{v_3}}{N_{v_2}}\right), \tag{B3}$$

provided that $M_{B_2}/M_{A_2}=M_{B_1}/M_{A_1}=1$. This will be true in the photon energy range where $\alpha(h\nu)$ is a slowly varying function of $(h\nu)$. Multiplication of Eq. (17) by Eq. (18) results in the relation

$$\frac{B_1B_2}{A_1A_2}=\left(\frac{K_B/\alpha_B}{K_A/\alpha_A}\right)^2\left(\frac{N_{v_3}}{N_{v_1}}\right). \tag{B4}$$

If N_{v_1} is taken as a reference value (assumed to be unity here), the ratios represent a calculated density of states (N_v) which differs from the measured density of states by powers of the ratio $[(K_B/\alpha_B)/(K_A/\alpha_A)]$. This ratio can be replaced by an exponential so that

$$\frac{K_B/\alpha_B}{K_A/\alpha_A}=\exp(a\Delta E), \tag{B5}$$

where $\Delta E=h\nu_B-h\nu_A$. By using Eq. (B5), Eqs. (B2) and (B4) can be written

$$N_{v_2}'=B_2/A_2=N_{v_2}\exp[a(E_{v_2}-E_{v_1})], \tag{B6}$$

$$N_{v_3}'=B_2/A_2=N_{v_3}\exp[a(E_{v_3}-E_{v_1})]. \tag{B7}$$

Going over to a continuous variable E_0 to designate the energy in the valence band, and assuming $E_{v_1}=0$, i.e., taking the zero of energy at the top of the valence band, gives

$$N_v'(E)=N_v(E)\exp(-aE). \tag{B8}$$

In order to obtain the conduction-band density of states, the ratios B_2/A_1 and B_1/A_0 given by

$$\frac{B_2}{A_1}=\left(\frac{K_B/\alpha_B}{K_A/\alpha_A}\right)\left(\frac{M_{B_2}}{M_{A_1}}\right), \tag{B9}$$

$$\frac{B_1}{A_0}=\left(\frac{K_B/\alpha_B}{K_A/\alpha_A}\right)\left(\frac{M_{B_1}}{M_{A_0}}\right), \tag{B10}$$

are used. Thus, the values of the quantity

$$M(E,h\nu)=T(E)S(E,h\nu)N_c(E) \tag{B11}$$

can be determined by a method completely analogous to that used to determine the valence-band density of states. The resulting expression, using the threshold energy E_B+E_A as the reference, is

$$M_c'(E)=M_c(E)\exp\{a[E-(E_G+E_A)]\}. \tag{B12}$$

APPENDIX C: EFFECTS OF ELECTRON-ELECTRON SCATTERING

Electron-electron scattering resulting in pair production can distort energy-distribution curves in photoemission from semiconductors. Berglund and Spicer[1] have developed an approximate theory for electron-electron scattering in metals which considers once-scattered electrons. This theory is based on the assump-

tion that the mean free path for inelastic scattering by pair production is much shorter than the absorption length and the mean free path for elastic scattering. Experimental evidence from photoemission curves on CdS indicates that many features of the above theory may apply to semiconductors at electron energies sufficiently high so that the assumptions apply.

In scattering via pair production, an electron in the conduction band with energy E' scatters to a conduction-band energy E by exciting an electron in the valence band with energy E_0 to an energy $E_0+(E'-E)$ in the conduction band. It will be assumed here that conservation of $\mathbf{k}$ is not an important selection rule in these transitions and that the matrix elements are constant, i.e., transition is assumed to occur with a probability proportional to the product of the densities of states. Thus, the probability $p_s(E',E)$ of scattering from an energy E' to an energy E is given by

$$p_s(E',E)=K\int_0^\infty N_c(E)N_v(E_0)N_c(E_0+E'-E)dE_0, \quad \text{(C1)}$$

with the total probability of scattering from energy E' given by

$$P_s(E')=\int_0^\infty p_s(E',E)dE \quad \text{(C2)}$$

if K is assumed to be independent of energy. Berglund and Spicer have shown that the energy distribution of photoemitted electrons becomes

$$N(E)=K_4\left\{\frac{1}{\alpha+[1/L(E)]}\right\} \times\left[\alpha'(E)+2\int_E^{h\nu}\frac{p_s(E',E)}{P_s(E')}\alpha'(E')dE'\right], \quad \text{(C3)}$$

where K_4 is assumed to be constant. The energy distribution of scattered primary electrons, as well as excited secondary electrons, is indicated by the second term in the brackets in Eq. (C3). This term represents the generation rate as a function of energy for once-scattered electrons and secondary electrons in the solid. In this paper, this generation term is used to estimate the energy distribution of electrons due to inelastic scattering.